Universität Karlsruhe (TH)
Institut für Baustatik

On the performance of enhanced strain finite elements in large strain deformations of elastic shells. Comparison of two classes of constitutive models for rubber materials

C. Sansour, S. Feih, W. Wagner

Mitteilung 5(2003)

Universität Karlsruhe (TH)
Institut für Baustatik

On the performance of enhanced strain finite elements in large strain deformations of elastic shells. Comparison of two classes of constitutive models for rubber materials

C. Sansour, S. Feih, W. Wagner

Mitteilung 5(2003)

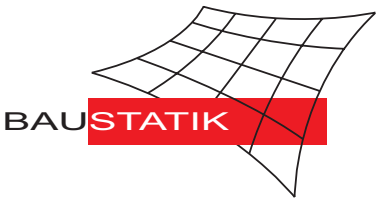

Prof. Dr.–Ing. W. Wagner
Institut für Baustatik
Universität Karlsruhe
Postfach 6980
76128 Karlsruhe

Telefon: (0721) 608–2280
Telefax: (0721) 608–6015
E–mail: bs@.uni-karlsruhe.de
Internet: http://www.bs.uni-karlsruhe.de

On the performance of enhanced strain finite elements in large strain deformations of elastic shells. Comparison of two classes of constitutive models for rubber materials

Carlo Sansour* , Stefanie Feih** , Werner Wagner***

*Dynamical Modelling and Simulation Group, School of Petroleum Engineering, University of Adelaide, Adelaide SA 5005, Australia
carlo.sansour@adelaide.edu.au

**RISØ National Laboratory, Materials Research Department, Roskilde, Denmark
stefanie.feih@risoe.dk

***Institut für Baustatik, Universität Karlsruhe,
Kaiserstr. 12, D-76131 Karlsruhe, Germany
wagner@bs.uni-karlsruhe.de

Abstract

This paper is concerned with the performance of shell finite elements, well established in locking free computations with linear constitutive laws, in the case of nonlinear elastic material behaviour. Specifically enhanced strain elements are focused on. It is shown that the element beahviour does depend on the resulting form of the stress tensor. Phenomenological models for highly nonlinear and elastically deforming rubber, like that of Odgen, are compared with the statistical-based constitutive model developed by Arruda and Boyce. Whereas computations with the Odgen, or any equivalent phenomenological model, prove unstable, the behaviour of the enhanced elements, when the statistical model is applied, is shown to be superior. The behaviour is attributed to the mathematical form of the resulting stress tensor.

Keywords: Enhanced finite elements, large elastic strains, shell computations.

1 Introduction

Modelling of material behaviour at large elastic strains as well as corresponding numerical computations is a field of great interest and is of various practical applications. The behaviour of rubber is perhaps the most known example which was studied at depth over the years. The so-called neo-Hookian law is the most simple form to describe such a behaviour. The Mooney-Rivlin law is a more accurate extension where the free energy function is assumed to depend on two invariants only. For many years the experiments of Treloar [13] have been a reference to model the behaviour of rubber. With the model of Ogden [7] a significantly accurate model was achieved and the mentioned experiments have been detected with sufficient accuracy up to elongation rate of 6. The constitutive model of Ogden (see e.g. [7]) exhibits two basic characteristics: 1) it is mathematically sound with the resulting field equations being elliptic and, 2) it is formulated in terms of eigen values of the stretch tensor. The second feature has direct impact on the numerical schemes to be adopted within a solution procedure. The formulation in the eigen values makes the computation of the tangent matrix an extensive task as second derivatives of the free energy function with respect

to the right Cauchy-Green strain tensor are to be evaluated. The task becomes even more involved once third derivatives become necessary as in the case of optimization problems.

With an eye on implementation, a formulation of constitutive laws for finite strain hyperelasticity in terms of the invariants of the right Cauchy-Green tensor circumvents the mentioned difficulties as 1) the evaluation of the derivative at any order is straightforward and 2) the formulation is not restricted to isotropic material behaviour. Such an approach has been followed in e.g. Sansour [9] where eight terms in the invariants have been considered. The model proved to be very accurate in the sense of reproducing the experimental results mentioned above. However, the simplicity was achieved at the cost of the loss of ellipticity of the governing equations at very high strain values, in fact an undesirable feature.

A common feature of the models mentioned so far is the inclusion of phenomenological material constants which are predicted by reproducing a specific set of experiments. Usually the experimental data considered is limited in many respects: uni-axial stretch, bi-axial stretch, and shear. One hopes that the model parameters evaluated, using a specific set of experiments, are universally valid and can predict a case of arbitrary deformation as well. In fact, given a specific set of experiments one may predict very accurately the measured response using e.g. an Ogden model or alternatively an equivalent model by determining the model parameters using the set of experiments at hand. Once the material parameters are fixed there is no guarantee, anyhow, that the same accuracy can be achieved for an arbitrary case of deformation.

A completely different philosophy is followed by the statistically-based constitutive models as developed e.g. by Arruda and Boyce [2]. The model predicts the highly nonlinear rubber material response using three constants only. The parameters have direct physical meaning and are as such independent of the specific kind of an experiment. They can be determined in one simple compressive test. The model of Arruda and Boyce is especially attractive for simulation purposes as well, due to the fact that physical and mathematical soundness is combined with simplicity. The stored energy function is formulated in terms of only the first invariant of the Cauchy-Green tensor. By that the resulting expression for the stress tensor becomes very much the same as that of linear elasticity with the significant difference that the shear modulus is deformation dependent. Accordingly, mathematically, the stress tensor takes a form well known from linear constitutive equations, a fact which seems to have impact in conjunction with the finite element formulation to be addressed next.

On the side of computations it is well documented that thin structures exhibit various locking phenomena when low dimensional finite elements are used. The experience is well established when constitutive laws with two material parameters (e.g. Young's modulus and Poisson ratio) are considered. Membrane, shear, and thickness locking observed in shell computations motivated intensive research leading to mixed formulations which proved capable of circumventing locking. Hybrid stress, hybrid strain, assumed, and enhanced strain finite element have been intensively developed and discussed in the literature. In Betsch and Stein [4], Klinkel and Wagner [6], Bischoff and Ramm [5] combinations of an assumed strain ansatz for the shear and transversal normal strains, and enhanced strains for the membran strains have been adopted. In Sansour [8] hybrid stress methods have been successfully developed. Contrasting this in Sansour and Kollmann [10] an enhanced strain model was considered. A comparison of these models for 4-node and 9-node elements including a strain hybrid method can be found in Sansour and Kollmann [11].

Whereas hybrid stress and enhanced strain elements proved to be equivalent in the case of linear elastic laws (within regular meshes), the enhanced strain concept is a strain-based formulation and can be well applied when the constitutive law is not linear and a Legendre transformation is not available. An interesting observation reported in [9] is that the application of nonlinear constitutive laws of the Ogden-type or an equivalent phenomenological model (such as the eight parameter model mentioned above) results in conjunction with the mentioned locking-free elements in totally unstable computations. In other words, those elements, well developed and successfully applied using linear constitutive laws, failed completely in shell computations when nonlinear constitutive laws of the mentioned type are considered.

The question now arises, whether this experience is generally valid for any nonlinear elastic constitutive law or whether it is connected to the form of the constitutive law at hand. Recalling the fact that the statistical model results in expressions mathematically very much the same as those of the linear constitutive law, the model is an ideal candidate to examine this question. Accordingly, the paper is concerned with the finite element computations of thin shells at large strains using the statistical model and an enhanced strain finite element formulation as compared to alternative models such as the eight-parameter one. In fact it is one of the basic results of this study that the raised question can be given a clear answer: the stability of the enhanced strain elements depends radically on the form of the constitutive law at hand. The application of the statistical model in conjunction with the enhanced strain elements results in superior behaviour. The deformation can be easily detected even in the regime of very high strains.

The paper is organized as follows. In sections 2, the constitutive models are briefly presented and in section 3, the expressions for the stress tensor as well as the material tangent are derived. Section 4 summarizes the shell theory and in section 5 the numerical results are presented. The paper closes with a discussion.

2 The constitutive model

Let $\mathbf{F}$ be the deformation gradient, $\mathbf{C} = \mathbf{F}^{\mathrm{T}}\mathbf{F}$ the right Cauchy-Green strain tensor. The class of elastic materials being interesting for this work is characterized by the well established volumetric-isochoric split. The developed constitutive equations are functions of the invariants of $\mathbf{C}$ which are defined by

$$I_1 = \mathrm{tr}\mathbf{C}, \qquad I_2 = \frac{1}{2}\left[(\mathrm{tr}\mathbf{C})^2 - \mathrm{tr}\mathbf{C}^2\right], \qquad I_3 = \det \mathbf{C}\ , \tag{1}$$

where the operator tr denotes the trace operation and det is the determinant of a tensor.

For the volumetric-isochoric split it is convenient to define the modified invariants

$$\bar{I}_1 = \frac{I_1}{I_3^{\frac{1}{3}}}, \qquad \bar{I}_2 = \frac{I_2}{I_3^{\frac{2}{3}}}\ , \tag{2}$$

because these allow for a purely isochoric deformation.

In what follows we briefly describe only the statistical model and the 8 parameter model. The Odgen model will not be discussed as it is well established and well documented in the literature.

2.1 The statistical model

Many attempts for phenomenological models of rubber deformation have been developed and a summary of those is given by Treloar [13]. However, most of these models do not try to link the adjustable parameters to any physical deformation mechanism or are not able to predict the behaviour of rubber material sufficiently well.

The implemented constitutive relation by Arruda, Boyce [2] and Anand [1] is based on an eight-chain representation of the underlying macromolecular network structure of the rubber and the non-Gaussian behaviour of the individual chains in the network. The eight-chain model accurately captures the cooperative nature of network deformation and requires only two parameters: a shear modulus C_R and a parameter N describing the limiting extensibility of the chains. The chain extension reduces to a function of the root-mean-square of the principal applied stretches, therefore capturing the three-dimensional behaviour of the material. Langevin statistics are used to describe the limited extensibility of polymer chains during the elastic ext ension.

The energy storage function in compressible form is derived by Anand [1] (for explanation see also [2]) and can be formulated in terms of the modified first invariant and the determinant of the deformation gradient. Making use of the volumetric-isochoric split described above it follows

$$
\begin{aligned}
W &= W^{\text{iso}} + W^{\text{vol}} \quad \text{with} && (3)\\
W^{\text{iso}} &= C_R \left(\frac{1}{2}(\bar{I}_1 - 3) + \frac{1}{20N}(\bar{I}_1^2 - 9) + \frac{11}{1050N^2}(\bar{I}_1^3 - 27) \right. && (4)\\
&\quad \left. + \frac{19}{7000N^3}(\bar{I}_1^4 - 81) + \frac{519}{673750N^4}(\bar{I}_1^5 - 243) + \dots \right) \\
W^{\text{vol}} &= \frac{1}{2}\kappa(\ln \sqrt{I_3})^2 \quad , && (5)
\end{aligned}
$$

where C_R can be compared with the shear modulus, N describes the limiting extensibility of the polymer chains and κ the bulk modulus of the rubber material. The first two constants are based directly on physical deformation mechanisms. For the energy storage form the series expansion form of the inverse Langevin function is needed which can be found in [13].

Note that the energy storage function does not depend on the second invariant of the Cauchy-Green tensor. This fact is due to the basic idea of the statistically-based eight-chain material model. For further details and discussion of the model and its statistical background see [2].

2.2 An eight-parameter model

As an example of a model which takes different invariants into account we consider briefly an eight-parameter model the energy storage function of which is given as

$$
\begin{aligned}
W &= W^{\text{iso}} + W^{\text{vol}} \quad \text{with} && (6)\\
W^{\text{iso}} &= \alpha_1 \bar{I}_1 + \alpha_2 \bar{I}_2 + \alpha_3 \bar{I}_1^2 + \alpha_4 \bar{I}_1 \bar{I}_2 + \alpha_5 \bar{I}_1^3 + \alpha_6 \bar{I}_2^2 + \alpha_7 \bar{I}_1^4 + \alpha_8 \bar{I}_2^2 \bar{I}_1 && (7)\\
W^{\text{vol}} &= \alpha_9 (\ln \sqrt{I_3})^2. && (8)
\end{aligned}
$$

The constants α_1 to α_8 are the eight material parameters. They are determined with the help of the least squares method by comparing the theoretically resulting 1. Piola-Kirchhoff stresses with those stresses measured and reported by Treloar [13]. The values are determined by Sansour [9] and given below

$$
\begin{aligned}
\alpha_1 &= 0.1796 & \qquad \alpha_5 &= 0.3473 \times 10^{-4}\\
\alpha_2 &= 0.0145 & \qquad \alpha_6 &= -0.8439 \times 10^{-3}\\
\alpha_3 &= -0.1684 \times 10^{-2} & \qquad \alpha_7 &= 0.432 \times 10^{-7}\\
\alpha_4 &= 0.3268 \times 10^{-3} & \qquad \alpha_8 &= 0.5513 \times 10^{-5}\,.
\end{aligned}
$$

The parameter α_9 can again be seen as the bulk modulus. For further details and discussion of the model see [9]. It is to be stressed that the model does not preserve ellipticity in the very high strain regime. This issue is anyhow of less interest in this paper, as we are interested in discussing the stability aspects of enhanced strain elements depending on the form of the resulting stress tensor. For a sufficiently large range of strains the model is applicable and can be used to explore the mentioned question of stability.

3 Stress tensor and tangent operator

In this section a closed form of the derived tangent operator and stress tensor is given.

The second Piola-Kirchhoff stress tensor $\mathbf{S}$ can be calculated by finding the derivative of the energy storage function with respect to $\mathbf{C}$

$$
\mathbf{S} = 2\frac{\partial W}{\partial \mathbf{C}} = a_1 \mathbf{1} + a_2 \mathbf{C} + a_3 \mathbf{C}^{-1} \quad . \tag{9}
$$

Furthermore, the following expressions will be needed later on

$$
\begin{aligned}
\frac{\partial I_1}{\partial \mathbf{C}} &= \mathbf{1} && (10)\\
\frac{\partial I_2}{\partial \mathbf{C}} &= I_1 \mathbf{1} - \mathbf{C} && (11)\\
\frac{\partial I_3}{\partial \mathbf{C}} &= I_3 \mathbf{C}^{-1} \quad . && (12)
\end{aligned}
$$

The tangent matrix $\mathcal{D}$ can be determined like the stress tensor by calculating the second derivative of the energy storage function with respect to $\mathbf{C}$

$$
\mathcal{D} = \frac{\partial \mathbf{S}}{\partial \mathbf{C}} = 2\frac{\partial^2 W}{\partial \mathbf{C}\, \partial \mathbf{C}} \quad . \tag{13}
$$

3.1 The statistical model

Calculating the stress according to Eq. 9 leads to

$$\begin{aligned}
\mathbf{S} &= a_1\mathbf{1} + a_2\mathbf{C} + a_3\mathbf{C}^{-1} \quad \text{with} \\
a_1 &= 2C_R\left(\frac{1}{2} + \frac{1}{10N}\bar{I}_1 + \frac{11}{350N^2}\bar{I}_1^2 + \frac{19}{1750N^3}\bar{I}_1^3 \right. \\
&\quad \left. + \frac{519}{134750N^4}\bar{I}_1^4 + \ldots\right) I_3^{-\frac{1}{3}} \\
a_2 &= 0 \\
a_3 &= -\frac{2}{3}C_R\left(\frac{1}{2} + \frac{1}{10N}\bar{I}_1 + \frac{11}{350N^2}\bar{I}_1^2 + \frac{19}{1750N^3}\bar{I}_1^3 \right. \\
&\quad \left. + \frac{519}{134750N^4}\bar{I}_1^4 + \ldots\right)\bar{I}_1 + \kappa \ln\sqrt{I_3} \quad .
\end{aligned} \tag{14}$$

The expression for a_2 is zero as the energy storage function does not depend on the second invariant.

The tangent matrix can be determined according to Eq. 13. This leads to the following compact and closed form for the tangent matrix in index notation

$$\begin{aligned}
(\mathcal{D})^{ijrs} &= 2\Big[b_1(\boldsymbol{\delta})^{ij}(\boldsymbol{\delta})^{rs} + b_2\left((\mathbf{C}^{-1})^{ij}(\boldsymbol{\delta})^{rs} + (\boldsymbol{\delta})^{ij}(\mathbf{C}^{-1})^{rs}\right) \\
&\quad + (b_3+b_4)(\mathbf{C}^{-1})^{ij}(\mathbf{C}^{-1})^{rs} - (b_5+b_6)(\mathbf{C}^{-1})^{ir}(\mathbf{C}^{-1})^{sj}\Big]
\end{aligned} \tag{15}$$

with the following coefficients

$$\begin{aligned}
b_1 &= C_R I_3^{-\frac{1}{3}}\left[\frac{1}{10N} + \frac{11}{175N^2}\bar{I}_1 + \frac{57}{1750N^3}\bar{I}_1^2 + \frac{1038}{67375N^4}\bar{I}_1^3 \right. \\
&\quad \left. + \frac{59991}{8758750N^5}\bar{I}_1^4 + \cdots\right] \\
b_2 &= -\frac{1}{3}C_R I_3^{-\frac{1}{3}}\left[\frac{1}{2} + \frac{1}{5N}\bar{I}_1 + \frac{33}{350N^2}\bar{I}_1^2 + \frac{38}{875N^3}\bar{I}_1^3 \right. \\
&\quad \left. + \frac{519}{26950N^4}\bar{I}_1^4 + \cdots\right] \\
b_3 &= \frac{1}{9}C_R\left[\frac{1}{2}\bar{I}_1 + \frac{1}{5N}\bar{I}_1^2 + \frac{33}{350N^2}\bar{I}_1^3 + \frac{38}{875N^3}\bar{I}_1^4 + \frac{519}{26950N^4}\bar{I}_1^5 + \cdots\right] \\
b_4 &= \frac{\kappa}{4} \\
b_5 &= -\frac{1}{3}C_R\left(\frac{1}{2} + \frac{1}{10N}\bar{I}_1 + \frac{11}{350N^2}\bar{I}_1^2 + \frac{19}{1750N^3}\bar{I}_1^3 \right. \\
&\quad \left. + \frac{519}{134750N^4}\bar{I}_1^4 + \ldots\right)\bar{I}_1 \\
b_6 &= \frac{1}{2}\kappa \ln\sqrt{I_3} \quad .
\end{aligned}$$

Note that the material stress tensor related to the spatial Kirchhoff tensor is an Eshelby-like quantity defined by

$$\boldsymbol{\Xi} = \mathbf{CS}. \tag{16}$$

The Kirchhoff stress tensor $\boldsymbol{\tau}$ is then given as $\boldsymbol{\tau} = \mathbf{F}^{-T}\boldsymbol{\Xi}\mathbf{F}^{T}$ revealing the significance of $\boldsymbol{\Xi}$ as it shares with $\boldsymbol{\tau}$ the same invariants. From (16) and (14) one concludes

$$\boldsymbol{\Xi} = a_1\mathbf{C} + a_3\mathbf{1}, \tag{17}$$

and correspondingly,

$$\boldsymbol{\tau} = a_1\mathbf{b} + a_3\mathbf{1}, \tag{18}$$

where $\mathbf{b} = \mathbf{F}\mathbf{F}^{\mathrm{T}}$ being the left Cauchy-Green strain tensor. From the last two equations it is clear that, mathematically, the form of the equation is that of the linear theory with the only difference being that the parameters are not constant.

3.2 The eight-parameter model

The stress for this model can be calculated according to Eq. 9, to result in

$$\mathbf{S} = a_1\mathbf{1} + a_2\mathbf{C} + a_3\mathbf{C}^{-1}, \tag{19}$$

with

$$\begin{aligned}
a_1 &= 2I_3^{-\frac{1}{3}}\left(\alpha_1 + \alpha_2\bar{I}_1 + 2\alpha_3\bar{I}_1 + \alpha_4\bar{I}_1^2 + 3\alpha_5\bar{I}_1^2 + 4\alpha_7\bar{I}_1^3 + \alpha_4\bar{I}_2\right. \\
&\quad \left. +2\alpha_6\bar{I}_1\bar{I}_2 + 2\alpha_8\bar{I}_1^2\bar{I}_2 + \alpha_8\bar{I}_2^2\right)\ , \\
a_2 &= -2I_3^{-\frac{2}{3}}\left(\alpha_2 + \alpha_4\bar{I}_1 + 2\alpha_6\bar{I}_2 + 2\alpha_8\bar{I}_1\bar{I}_2\right)\ , \\
a_3 &= -\frac{2}{3}\left(\alpha_1\bar{I}_1 + 2\alpha_3\bar{I}_1^2 + 3\alpha_5\bar{I}_1^3 + 4\alpha_7\bar{I}_1^4 + 2\alpha_2\bar{I}_2 + 3\alpha_4\bar{I}_1\bar{I}_2 + \right. \\
&\quad \left. 4\alpha_6\bar{I}_2^2 + 5\alpha_8\bar{I}_1\bar{I}_2^2 - 3\alpha_9\ln(I_3)\right)\ .
\end{aligned}$$

The tangent matrix is calculated by Eq. 13 resulting in the following expression

$$\begin{aligned}
(\mathcal{D})^{ijrs} &= b_1(\mathbf{C}^{-1})^{ij}(\mathbf{C}^{-1})^{rs} + b_2\left[(\mathbf{C})^{ij}(\mathbf{C}^{-1})^{rs} + (\mathbf{C}^{-1})^{ij}(\mathbf{C})^{rs}\right] + \\
&\quad b_3\left[(\mathbf{C}^{-1})^{ij}(\boldsymbol{\delta})^{rs} + (\boldsymbol{\delta})^{ij}(\mathbf{C}^{-1})^{rs}\right] + b_4(\mathbf{C})^{ij}(\mathbf{C})^{rs} + b_5\left[(\mathbf{C})^{ij}(\boldsymbol{\delta})^{rs} + \right. \\
&\quad \left.(\boldsymbol{\delta})^{ij}(\mathbf{C})^{rs}\right] + b_6(\boldsymbol{\delta})^{ij}(\boldsymbol{\delta})^{rs} + a_2(\boldsymbol{\delta})^{ir}(\boldsymbol{\delta})^{js} - a_3(\mathbf{C}^{-1})^{ir}(\mathbf{C}^{-1})^{sj}\quad .
\end{aligned} \tag{20}$$

The factors $b_1 \ldots b_6$ are

$$\begin{aligned}
b_1 &= \frac{2}{9}\left(\alpha_1\bar{I}_1 + 4\alpha_1\bar{I}_1^2 + 9\alpha_5\bar{I}_1^3 + 16\alpha_7\bar{I}_1^4 + 4\alpha_2\bar{I}_2 + 9\alpha_4\bar{I}_1\bar{I}_2\right. \\
&\quad \left. +16\alpha_6\bar{I}_2^2 + 25\alpha_8\bar{I}_1\bar{I}_2^2 + 9\alpha_9\right), \\
b_2 &= \frac{2}{3}I_3^{-\frac{2}{3}}\left(2\alpha_2 + 3\alpha_2\bar{I}_1 + 8\alpha_6\bar{I}_2 + 10\alpha_8\bar{I}_1\bar{I}_2\right), \\
b_3 &= -\frac{4}{3}\left(\alpha_1 + 2\alpha_2\bar{I}_1 + 4\alpha_3\bar{I}_1 + 3\alpha_4\bar{I}_1^2 + 9\alpha_5\bar{I}_1^2 + 16\alpha_7\bar{I}_1^3\right. \\
&\quad \left. 3\alpha_4\bar{I}_2 + 8\alpha_6\bar{I}_1\bar{I}_2 + 10\alpha_8\bar{I}_1^2\bar{I}_2 + 5\alpha_8\bar{I}_2^2\right), \\
b_4 &= 2I_3^{-\frac{4}{3}}\left(2\alpha_6 + 2\alpha_8\bar{I}_1\right),
\end{aligned}$$

$$
\begin{aligned}
b_5 &= -2I_3^{-1}\left(\alpha_4 + 2\alpha_6\bar{I}_1 + 2\alpha_8\bar{I}_1^2 + 2\alpha_8\bar{I}_2\right), \\
b_6 &= 2I_3^{-\frac{2}{3}}\left(\alpha_2 + 2\alpha_3 + 3\alpha_4\bar{I}_1 + 6\alpha_5\bar{I}_1 + 2\alpha_6\bar{I}_1^2 + 12\alpha_7\bar{I}_1^2 + 2\alpha_8\bar{I}_1^3\right. \\
&\quad \left. +2\alpha_6\bar{I}_2 + 6\alpha_8\bar{I}_1\bar{I}_2\right).
\end{aligned}
$$

Recalling (16), the material stress tensor takes the form

$$
\boldsymbol{\Xi} = a_1\mathbf{C} + a_2\mathbf{C}^2 + a_3\mathbf{1}\,. \tag{21}
$$

A comparison with (19) reveals that, beyond the scalar values of a_1 and a_3, it is the term quadratic in $\mathbf{C}$ which constitutes the difference. It is also this term which makes the difference to a linear constitutive law which as well known depends on two scalar (but constant) elastic parameters.

4 Summary of the shell theory

In what follows we summarize the basic issues of the shell theory adopted. For detailed description of the theory we refer to [8, 9].

The shell theory is based on the following fundamental assumption. We assume that any configuration of the shell space is determined by the equation

$$
\mathbf{x}(\vartheta^\alpha, z) = \mathbf{x^0}(\vartheta^\alpha) + (z + z^2\chi(\vartheta^\alpha))\mathbf{a}_3(\vartheta^\alpha), \tag{22}
$$

where z is the co-ordinate in thickness direction and $\mathbf{x^0}$ denotes a configuration of the mid-surface. By that the ordered triple $(\mathbf{x^0}, \mathbf{a}_3, \chi)$ defines the configuration space of the shell.

The assumed shell kinematics is the simplest possible which allows for a linear distribution of the transverse strains over the shell thickness. Consequently, three-dimensional constitutive equations can be applied. Accordingly, the formulation is suitable for small as well as for large strain cases in elasticity or elasto-viscoplasticity . Restricting ourselves to only linear terms in z, the right Cauchy Green strain tensor of the shell space $\mathbf{C}$ takes the additive form

$$
\mathbf{C} = \mathbf{C^0} + z\mathbf{K}. \tag{23}
$$

$\mathbf{C^0}$ relates to the shell mid-surface and is independent of z.

At the shell mid-surface the triple $\mathbf{A}_\alpha, \mathbf{N}, (\alpha = 1, 2)$ defines the natural covariant base. At any point in the shell space, the natural covariant base vectors are given by $\mathbf{G}_\alpha, \mathbf{N}, (\alpha = 1, 2)$. The relation holds $\mathbf{G}_\alpha = \mathbf{J}\mathbf{A}_\alpha$, where the two-dimensional tensor $\mathbf{J}$ defines the so-called schifter tensor which is determined by the geometry and the curvature of the shell: $\mathbf{J} = \mathbf{1} - z\mathbf{B}$ with $\mathbf{B}$ being the curvature tensor. Introducing the displacement field $\mathbf{u^0}$ and the difference vector $\mathbf{w}$ according to

$$
\mathbf{u^0} : = \mathbf{x^0} - \mathbf{X^0}, \tag{24}
$$

$$
\mathbf{w} : = \mathbf{a}_3 - \mathbf{N}, \tag{25}
$$

where $\mathbf{X^0}$ defines a reference configuration of the mid-surface, and considering the following decompositions

$$\mathbf{C^0} = C_{\alpha\beta}\mathbf{A}^\beta \otimes \mathbf{A}^\alpha + C_{3\alpha}\mathbf{A}^\alpha \otimes \mathbf{N} + C_{\alpha 3}\mathbf{N} \otimes \mathbf{A}^\alpha + C_{33}\mathbf{N} \otimes \mathbf{N}, \tag{26}$$

$$\mathbf{K} = K_{\alpha\beta}\mathbf{A}^\beta \otimes \mathbf{A}^\alpha + K_{3\alpha}\mathbf{A}^\alpha \otimes \mathbf{N} + K_{\alpha 3}\mathbf{N} \otimes \mathbf{A}^\alpha + K_{33}\mathbf{N} \otimes \mathbf{N}, \tag{27}$$

one arrives at the following expressions

$$\begin{aligned}
C_{\alpha\beta} &= A_{\alpha\beta} + \mathbf{A}_\beta \cdot \mathbf{u}^{\mathbf{0}}_{,\alpha} + \mathbf{A}_\alpha \cdot \mathbf{u}^{\mathbf{0}}_{,\beta} + \mathbf{u}^{\mathbf{0}}_{,\alpha} \cdot \mathbf{u}^{\mathbf{0}}_{,\beta}, && (28)\\
C_{\alpha 3} &= \mathbf{N} \cdot \mathbf{u}^{\mathbf{0}}_{,\alpha} + \mathbf{A}_\alpha \cdot \mathbf{w} + \mathbf{u}^{\mathbf{0}}_{,\alpha} \cdot \mathbf{w}, && (29)\\
C_{3\alpha} &= C_{\alpha 3}, && (30)\\
C_{33} &= 1 + 2\mathbf{N} \cdot \mathbf{w} + \mathbf{w} \cdot \mathbf{w}, && (31)\\
K_{\alpha\beta} &= B_{\alpha\beta} + 2(\mathbf{N}_{,\alpha} \cdot \mathbf{u}^{\mathbf{0}}_{,\beta} + \mathbf{N}_{,\beta} \cdot \mathbf{u}^{\mathbf{0}}_{,\alpha} + \mathbf{A}_\alpha \cdot \mathbf{w}_{,\beta} + \mathbf{A}_\beta \cdot \mathbf{w}_{,\alpha} + \mathbf{u}^{\mathbf{0}}_{,\alpha} \cdot \mathbf{w}_{,\beta} + \mathbf{u}^{\mathbf{0}}_{,\beta} \cdot \mathbf{w}_{,\alpha}), && (32)\\
K_{\alpha 3} &= (\mathbf{N}_{,\alpha} \cdot \mathbf{w} + \mathbf{N} \cdot \mathbf{w}_{,\alpha} + \mathbf{w} \cdot \mathbf{w}_{,\alpha}) + \mathbf{2}\chi(\mathbf{A}_\alpha \cdot \mathbf{w} + \mathbf{N} \cdot \mathbf{u}^{\mathbf{0}}_{,\alpha} + \mathbf{w} \cdot \mathbf{u}^{\mathbf{0}}_{,\alpha}), && (33)\\
K_{33} &= 4\chi(1 + 2\mathbf{N} \cdot \mathbf{w} + \mathbf{w} \cdot \mathbf{w}), && (34)
\end{aligned}$$

to be considered as the dominating strain measures of the shell.

The principle of virtual displacement in three dimensions reads

$$\int_{\mathcal{B}} \frac{1}{2}\mathbf{S} : \delta\mathbf{C}\, dV - \int_{\mathcal{B}} \mathbf{f} \cdot \delta\mathbf{x}\, dV - \int_{\partial\mathcal{B}} \mathbf{t} \cdot \delta\mathbf{x}\, dS = 0, \tag{35}$$

where the scalar product of tensors is denoted by the use of (:), $\mathcal{B}$ denotes the shell body, $\partial\mathcal{B}$ its boundary, dV and dS are the volume and surface elements, respectively, $\mathbf{f}, \mathbf{t}$ are the body and the surface forces, respectively. The relation holds $dV = Jd\sigma dz$, with J denoting $\det\mathbf{J}$, the determinant of the shifter, and with $d\sigma$ being a surface element of the shell mid-surface. We further denote the shell thickness by h and its mid-surface by $\mathcal{M}$. We assume that the shell mid-surface has a smooth curve $\partial\mathcal{M}$ as a boundary, with the parameter length s and the external normal vector $\boldsymbol{\nu}$. The boundary of the shell consists of three parts: an upper ($z = h/2$), a lower ($z = -h/2$), and a lateral surface. If we denote the upper surface by $\partial\mathcal{B}^+$, the lower one by $\partial\mathcal{B}^-$ and the lateral one by $\partial\mathcal{B}^s$ and make use of the notation $J^+ = J|_{z=h/2}, J^- = J|_{z=-h/2}$, and J^s for J at the lateral surface, we may write for the surface elements $dS^+ = J^+ d\sigma, dS^- = J^- d\sigma$ and $dS^s = J^s dz ds$.

First let us consider the external virtual work of the shell space

$$\delta\mathcal{W}_{ext} := \int_{\mathcal{B}} \mathbf{f} \cdot \delta\mathbf{x}\, dV + \int_{\partial\mathcal{B}} \mathbf{t} \cdot \delta\mathbf{x}\, dS\,. \tag{36}$$

With the definitions

$$\begin{aligned}
\mathbf{p}: &= \int_{-h/2}^{h/2} \mathbf{f} J\, dz + J^+\mathbf{t}^+ + J^-\mathbf{t}^-, && (37)\\
\mathbf{l}: &= \int_{-h/2}^{h/2} z\mathbf{f} J\, dz + \frac{h}{2}J^+\mathbf{t}^+ - \frac{h}{2}J^-\mathbf{t}^-, && (38)\\
\mathbf{p}^s: &= \int_{-h/2}^{h/2} \mathbf{t}^s J^s\, dz, && (39)\\
\mathbf{l}^s: &= \int_{-h/2}^{h/2} z\mathbf{t}^s J^s\, dz, && (40)
\end{aligned}$$

Eq. (36) reduces to

$$\delta\mathcal{W}_{ext} \;=\; \int_{\mathcal{M}} \left(\mathbf{p}\cdot\delta\mathbf{x^0}+\mathbf{l}\cdot\delta\mathbf{a}_3\right) d\sigma + \int_{\partial\mathcal{M}} \left(\mathbf{p}^s\cdot\delta\mathbf{x^0}+\mathbf{l}^s\cdot\delta\mathbf{a}_3\right) ds \tag{41}$$

as the two dimensional form of the external power. Higher order terms which include also those related to χ have been neglected.

To consider the internal virtual power we define first the pull-back of $\mathbf{S}$ under $\mathbf{J}$ which gives a stress tensor defined with respect to the mid-surface

$$\mathbf{S^0} = \mathbf{J}^{-1}\mathbf{S}\mathbf{J}^{-T}. \tag{42}$$

Note that $\mathbf{S^0}$ is still z-dependent. With the definitions

$$\mathbf{n}: \;=\; \frac{1}{2}\int_{-h/2}^{+h/2} \mathbf{S^0}\, J\, dz = \int_{-h/2}^{+h/2} \mathbf{J}^{-1}\frac{\partial \mathrm{W}(\mathbf{C})}{\partial \mathbf{C}}\mathbf{J}^{-T}\, J\, dz, \tag{43}$$

$$\mathbf{m}: \;=\; \frac{1}{2}\int_{-h/2}^{+h/2} z\mathbf{S^0}\, J\, dz = \int_{-h/2}^{+h/2} z\mathbf{J}^{-1}\frac{\partial \mathrm{W}(\mathbf{C})}{\partial \mathbf{C}}\mathbf{J}^{-T}\, J\, dz, \tag{44}$$

where (9) has been used, the principle of virtual power takes the final form

$$\int_{\mathcal{M}}(\mathbf{n}:\delta\mathbf{C^0}+\mathbf{m}:\delta\mathbf{K})d\sigma - \int_{\mathcal{M}} \left(\mathbf{p}\cdot\delta\mathbf{x^0}+\mathbf{l}\cdot\delta\mathbf{a}_3\right) d\sigma - \int_{\partial\mathcal{M}} \left(\mathbf{p}^s\cdot\delta\mathbf{x^0}+\mathbf{l}^s\cdot\delta\mathbf{a}_3\right) ds \;=\; 0. \tag{45}$$

Contrasting the external power, and in order to allow for the use of highly nonlinear constitutive equations and to avoid cumbersome estimations of the leading terms depending on powers in z, the elaboration of (43) and (44) is carried out, in practical computations, numerically.

5 An enhanced strain finite element

According to the concept of enhanced strains the strain tensor itself is enhanced (see e.g. [12]). We consider, accordingly, the following enhanced functional:

$$\delta\int_{\mathcal{B}} \mathrm{W}(\mathbf{C}+\tilde{\mathbf{C}})dV - \int_{\mathcal{M}} \left(\mathbf{p}\cdot\delta\mathbf{x^0}+\mathbf{l}\cdot\delta\mathbf{a}_3+\right) d\sigma - \int_{\partial\mathcal{M}} \left(\mathbf{p}^s\cdot\delta\mathbf{x^0}+\mathbf{l}^s\cdot\delta\mathbf{a}_3\right) ds = 0. \tag{46}$$

Whereas $\mathbf{C}$ in (46) is the strain measure of the shell space as defined by the relations (23) and (28)-(34), $\tilde{\mathbf{C}}$ is the independent enhanced strain field (incompatible field). The choice of the interpolation functions for $\tilde{\mathbf{C}}$ is crucial in order to arrive at well behaving elements. A guide to the formulation is the fact that it should be equivalent to the stress hybrid one when applied to the same class of problems (see [11] for details). Accordingly we restrict $\tilde{\mathbf{C}}$ to be of the form $\tilde{\mathbf{C}} = \mathbf{J}^{-T}\tilde{\mathbf{C}}^{\mathbf{0}}\mathbf{J}^{-1}$ where $\tilde{\mathbf{C}}^{\mathbf{0}}$ is independent of z. This is equivalent to an enhancement of the strains related to the mid-surface alone.

Since the enhanced strains are considered independent of the displacement field, Eq. (46) splits into the two equations

$$\int_{\mathcal{M}}(\mathbf{n}:\delta\mathbf{C^0}+\mathbf{m}:\delta\mathbf{K})d\sigma - \int_{\mathcal{M}} \left(\mathbf{p}\cdot\delta\mathbf{x^0}+\mathbf{l}\cdot\delta\mathbf{a}_3\right) d\sigma - \int_{\partial\mathcal{M}} \left(\mathbf{p}^s\cdot\delta\mathbf{x^0}+\mathbf{l}^s\cdot\delta\mathbf{a}_3\right) ds = 0, \tag{47}$$

and

$$\int_{\mathcal{M}} \mathbf{n} : \delta\tilde{\mathbf{C}}^{\mathbf{0}} d\sigma = 0, \tag{48}$$

where we have

$$\mathbf{n} : = \int_{-h/2}^{+h/2} \mathbf{J}^{-1} \frac{\partial \mathrm{W}(\mathbf{C}+\tilde{\mathbf{C}})}{\partial \mathbf{C}} \mathbf{J}^{-T} \, J \, dz, \tag{49}$$

$$\mathbf{m} : = \int_{-h/2}^{+h/2} z\mathbf{J}^{-1} \frac{\partial \mathrm{W}(\mathbf{C}+\tilde{\mathbf{C}})}{\partial \tilde{\mathbf{C}}} \mathbf{J}^{-T} \, J \, dz. \tag{50}$$

Note that the enhancement of the right Cauchy-green tensor is an additive one. The evaluation of (49) and (50) must be carried out numerically.

In accordance with (26) we consider the decomposition

$$\tilde{\mathbf{C}}^{\mathbf{0}} = \tilde{C}_{\alpha\beta}\mathbf{G}^{\alpha} \otimes \mathbf{G}^{\beta} + \tilde{C}_{\alpha 3}\mathbf{G}^{\alpha} \otimes \mathbf{N} + \tilde{C}_{3\alpha}\mathbf{N} \otimes \mathbf{G}^{\alpha} + \tilde{C}_{33}\mathbf{N} \otimes \mathbf{N}. \tag{51}$$

We restrict ourselves to four-noded elements. Accordingly all kinematical fields are interpolated using bi-linear interpolation functions. In computations using linear constitutive laws, the enhanced strain interpolation function proved to be of the following form (see again [11]):

$$\begin{aligned}
\tilde{C}_{11}(\xi,\eta) &= C_1\xi + C_2\xi\eta, && (52)\\
\tilde{C}_{22}(\xi,\eta) &= C_3\eta + C_4\xi\eta, && (53)\\
\tilde{C}_{33}(\xi,\eta) &= C_5\xi + C_6\eta + C_7\xi\eta, && (54)\\
\tilde{C}_{12}(\xi,\eta) &= C_8\xi + C_9\eta + C_{10}\xi\eta, && (55)\\
\tilde{C}_{13}(\xi,\eta) &= C_{11}\xi + C_{12}\xi\eta, && (56)\\
\tilde{C}_{23}(\xi,\eta) &= C_{13}\eta + C_{14}\xi\eta. && (57)\\
& && (58)
\end{aligned}$$

The fields $C_1....C_{12}$ are considered independent and are eliminated at the element level.

The introduction of interpolation functions of the displacement fields as well as of the enhanced strain fields in (47) and (48) leads to two coupled nonlinear sets of equations corresponding to the kinematical fields $(\mathbf{u}, \mathbf{w}, \chi)$ as well as to the enhanced strains $\tilde{\mathbf{C}}^{\mathbf{0}}$.

6 Numerical examples

Extensive numerical computations have been elaborated to identify the performance of the enhanced strain elements. Both material models, the statistical and the eight parameter model, have been applied. In addition, the well established model of Ogden was implemented as well (the model has not been discussed in the paper as it is well well known and established).

Both, the eight parameter model as well as the model of Ogden, result in a stress tensor which differs in its form from the linear elastic one. In both cases the enhanced strain computations exhibit poor convergence and stability characteristics. After the first converged

load steps, the convergence behaviour became so poor that very small steps where enforced rendering large strain computations impossible.

To the contrary, the element behaviour in the case of the statistical model, with the stress tensor having the same mathematical structure as that of linear elasticity, proved to be superior.

In order to make sure that the above mentioned behaviour is not restricted to a certain geometry or loading conditions, a large number of computations, documented in the following subsections, with different geometries and loading conditions was carried out. In all cases the following material parameter has been used: $N = 8.0$, $C_R = 1.56$ MPa, and $\kappa = 1000$ MPa. κ has been chosen fairly high in comparison with C_R to take into account the nearly incompressible behaviour during elastic deformation of rubber material.

6.1 Thin sheet under internal pressure

A thin sheet, fixed at its ends, is subject to internal pressure. One half of the sheet is modelled using 5×50 elements. The figures related to the problem definition, the load-displacement curve for the vertical displacement at the mid-point, and the final deformed configuration are given in the Figures 1-3.

6.2 Circular plate with hole under internal pressure

A circular plate with a hole is fixed at its outer boundary and subject to internal pressure. The problem definition is given in Fig. 4. 10×30 finite elements are considered for modelling the plate, where the 30 elements are taken in the radial direction. A load-displacement curve for the vertical displacement at the points at the inner radius is documented in Fig. 5, and the deformed configuration of the circular plate is captured in Fig. 6.

6.3 Circular plate with fixed hole under internal pressure

The same circular plate as in the previous example with same discretisation under the same internal pressure is considered now with the only difference being that the inner boundary is fixed as well. The response in this case is captured in the Figures 7-9. The load-displacement curve is given for a point with the radial co-ordinate being 0.11 m.

6.4 Cylinder with rigid diaphragm under internal pressure

Fig. 10 shows a cylinder with rigid diaphragm under internal pressure. The boundaries are free to move in the axial direction. One eighth of the cylinder is modelled using 16×16 elements. The load-displacement curve for the radial displacement at the mid of the cylinder (symmetry axes) is reproduced in Fig. 11, and the final deformed configuration in Fig. 12.

7 Discussion

In this paper the performance of an enhanced strain element formulation for shell computations at large elastic strains has been examined. Numerical experience shows clearly that the performance does depend on the mathematical expression for the stress tensor. Three models for rubber-like materials have been considered. The statistical model of Arruda and Boyce with the resulting stress tensor being of the same mathematical structure as that of linear elasticity, that is of the form $\boldsymbol{\sigma} = a_1\mathbf{1} + a_2\mathbf{C}$, proves well suited for enhanced strain formulations. In the non-linear case the scalars a_1, a_2 are simply not constant rather than deformation dependent. In contrast, the eight parameter model as well as the Odgen model resulted in unstable element performance.

As discussed in the introduction, other research groups have developed different shell element formulations to prevent locking in geometrically exact, but materially linear computations, such as the assumed strain formulations and various assumed-enhanced formulations (see references in introduction). It is interesting to note, that according to the experience of the authors, these elements exhibit the same behaviour as reported here with regard to the enhanced strain formulation.

Whether the computations remain stable for all possible and physically useful values of a_1 and a_2 remains an open question. The presented numerical examples as well as further ones not included in the paper, which incorporate a wide range of deformations, strongly suggest this. But a final statement can only be met on the basis of a rigorous mathematical analysis, which lies beyond the scope of the paper. Anyhow, it is hoped that this study will motivate one.

References

[1] Anand, L. (1996), "A constitutive Model for compressible elastomeric Solids", *Computational Mechanics*, **18**, pp. 339-355.

[2] Arruda, E.M. and Boyce, M. C. (1993), "A three-dimensional constitutive model for the large stretch behavior of rubber elastic material", *Journal of the Mechanics and Physics of Solids*, **41**, pp. 389-412.

[3] Bergström, J. S. und Boyce, M. C. (1998), "Constitutive Modeling of the large Strain time-dependent Behavior of Elastomers", Journal of the Mechanics and Physics of Solids, **46**(5), pp. 931-954.

[4] Betsch, P. and Stein, E. (1995), "An assumed strain approach avoiding artificial thickness straining for a non-linear 4-node shell element", *Comm. Num. Meth. Engrg.* **11**, 899-909.

[5] Bischoff, M. and Ramm, E. (1997), "Shear deformable shell elements for large strains and rotations", *Int. J. Numer. Meths. Engrg.* **40**, 4427-4449.

[6] Klinkel, S. and Wagner, W. (1997), "A geometrical non-linear brick element based on the EAS-method", *Int. J. Num. Meth. Eng.* **40**, 529-4545.

[7] Ogden, R.W. (1984), *Nonlinear Elastic Deformation*, Ellis Horwood Chichester.

[8] Sansour, C. (1995), "A theory and finite element formulation of shells at finite deformations involving thickness change: Circumventing the use of a rotation tensor", *Arch. Appl. Mech.* **65**, 194–216.

[9] Sansour, C. (1998), "Large Strain Deformations of elastic Shells. Constitutive Modeling and Finite Element Analysis", *Comp. Meth. Appl. Mech. Engrg.* **161**, pp. 1-18.

[10] Sansour, C. and Kollmann, F.G. (1998), "Large viscoplastic deformations of shells. Theory and finite element formulation", *Comput. Mechanics* **21**, 512-525.

[11] Sansour, C. and Kollmann, F.G. (2000), "Families of 4-node and 9-node finite elements for a finite deformation shell theory. An assessment of hybrid stress, hybrid strain, and enhanced strain elements", *Comput. Mechanics* **24**, 435-447.

[12] Simo, J.C. and Rifai, M.S. (1990), "A class of mixed assumed strain methods and the method of incompatible modes", *Int. J. Numer. Meths. Engrg.* **29**, 1595-1638.

[13] Treloar, L. R. G. (1975), *The Physics of Rubber Elasticity*, Clarendon Press, Oxford.

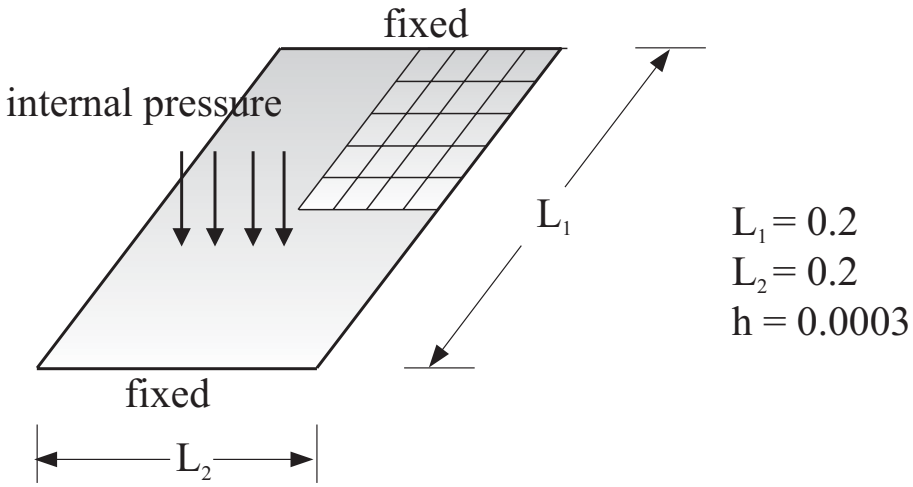

Fig. 1: Plate strip under internal pressure. Problem definition.

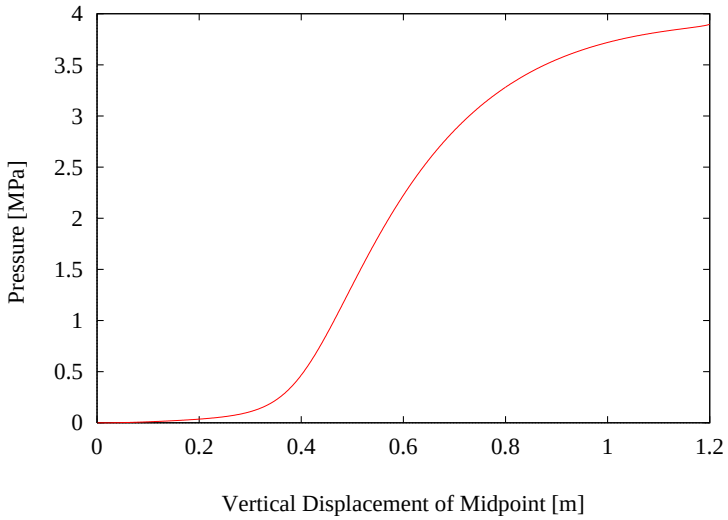

Fig. 2: Plate strip under internal pressure. Load-displacement curve

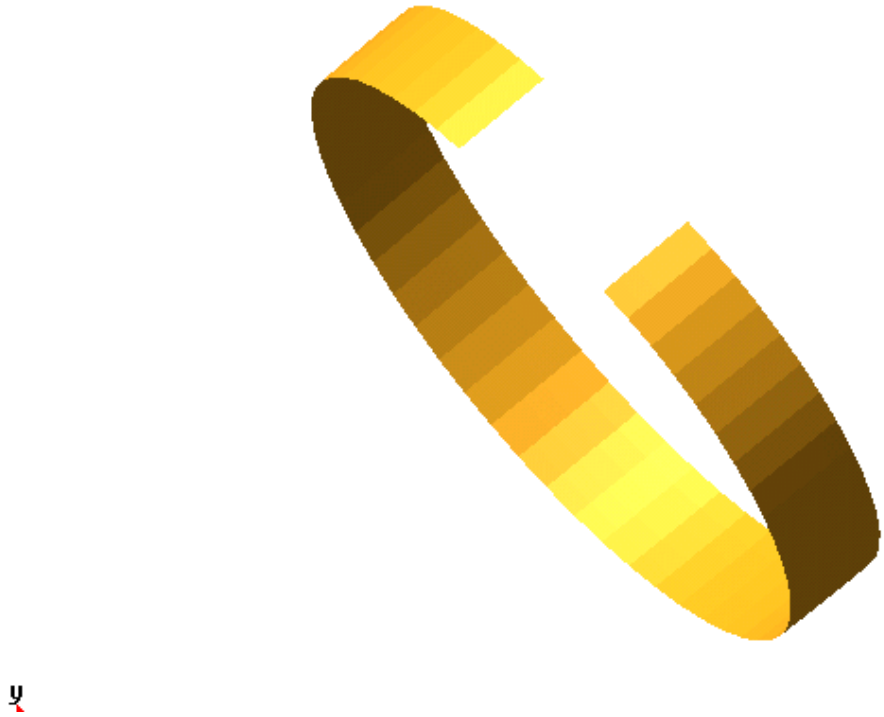

Fig. 3: Plate strip under internal pressure. Deformed configuration

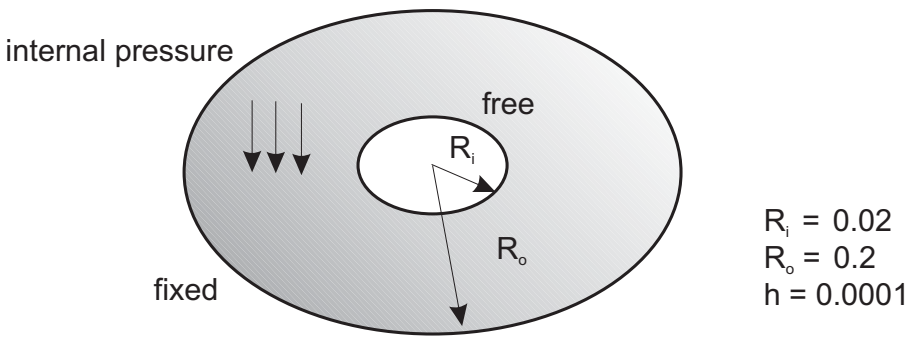

Fig. 4: Circular plate under internal pressure. Problem definition.

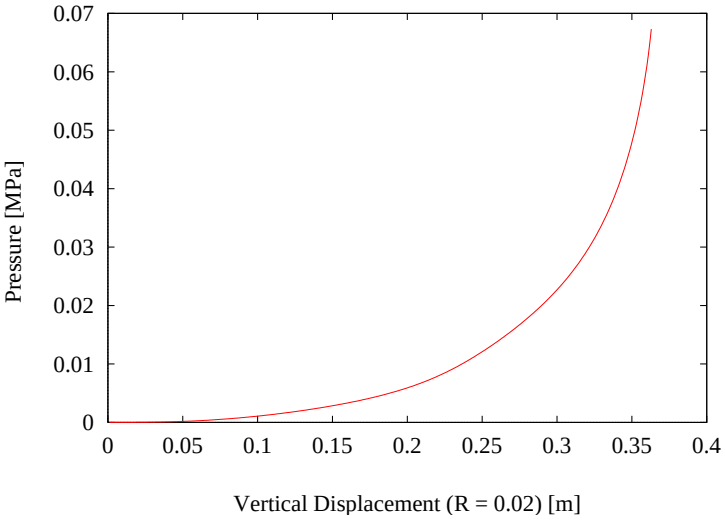

Fig. 5: Circular plate under internal pressure. Load-displacement curve

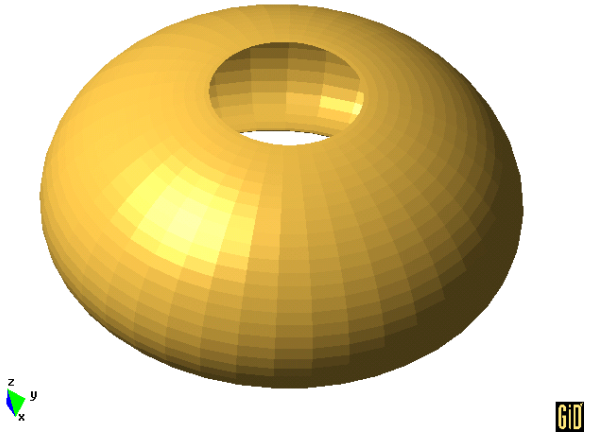

Fig. 6: Circular plate under internal pressure. Deformed configuration

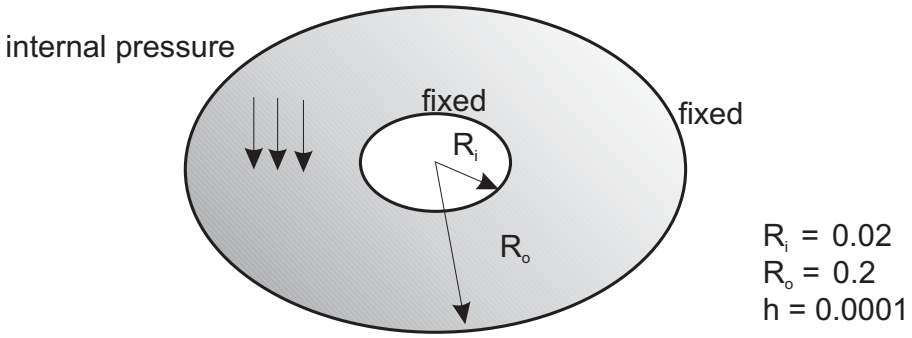

Fig. 7: Circular plate under internal pressure. Problem definition.

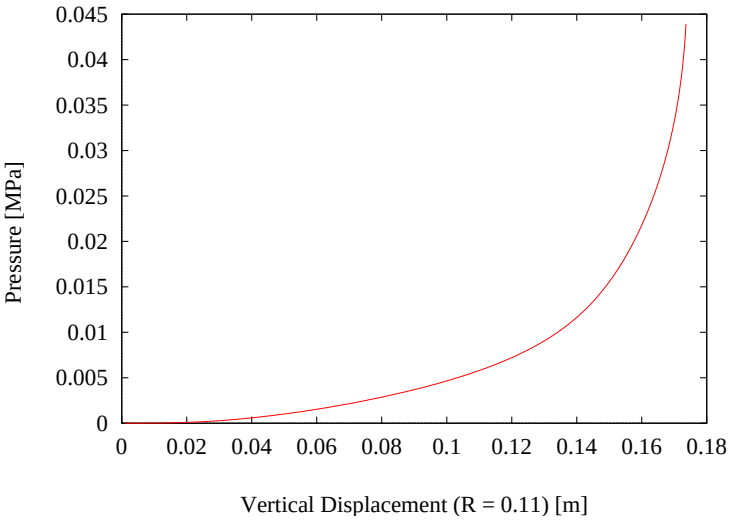

Fig. 8: Circular plate under internal pressure. Load-displacement curve

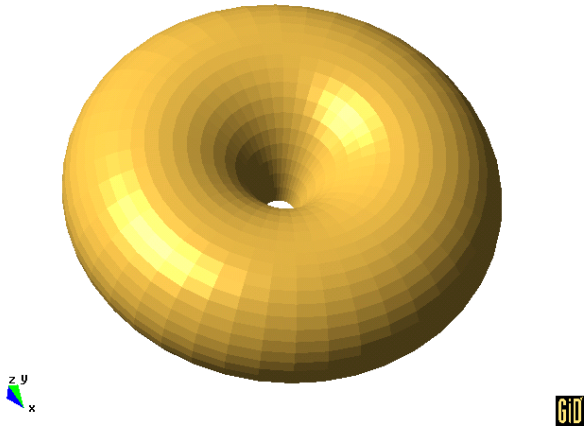

Fig. 9: Circular plate under internal pressure. Deformed configuration

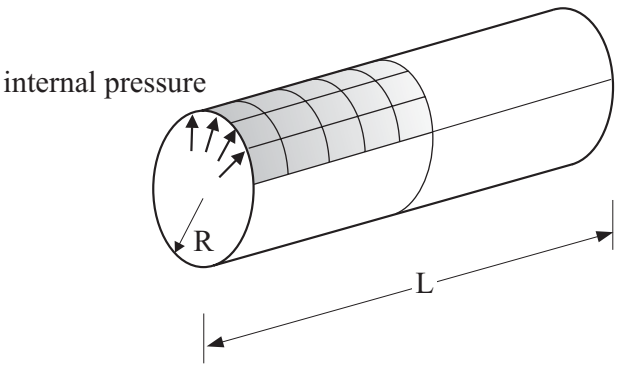

L = 0.2
R = 0.1
h = 0.001

Fig. 10: Cylinder under internal pressure. Problem definition.

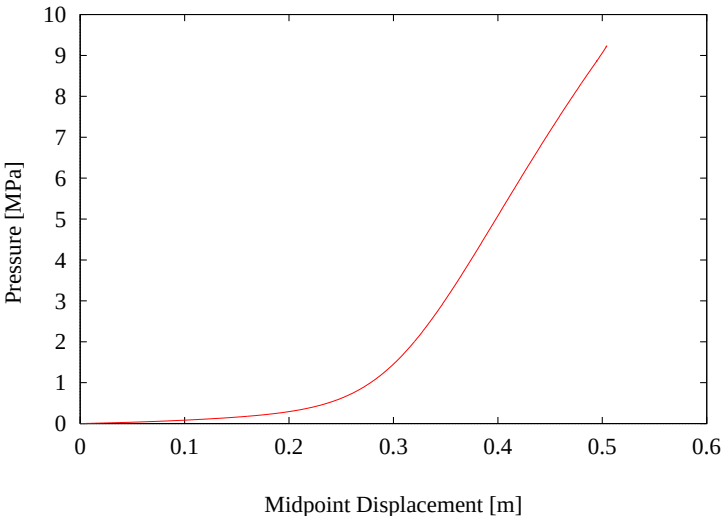

Fig. 11: Cylinder under internal pressure. Load-displacement curve

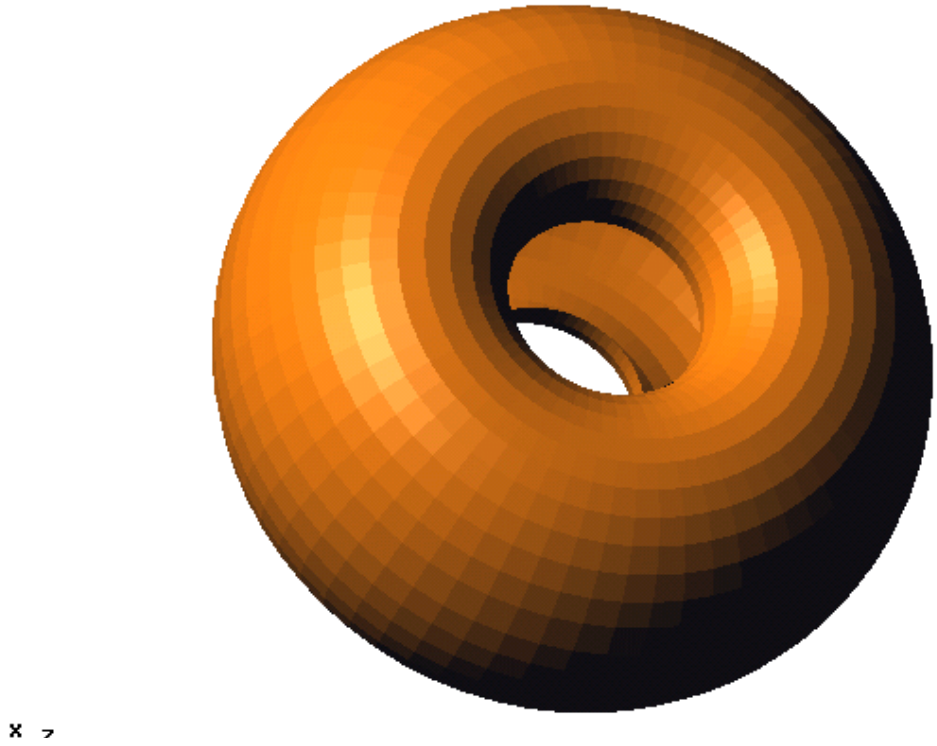

Fig. 12: Cylinder under internal pressure. Deformed configuration